High-precision spontaneous fission branching-ratio measurements for ^{240,242}Pu and ^{252}Cf isotopes

G. Bélier,[1,*] J. Aupiais,[1] G. Sibbens,[2] A. Moens,[2] and D. Vanleeuw[2]
[1]*CEA, DAM, DIF, F-91297 Arpajon, France*
[2]*EC-JRC.G.2 Retieseweg 111, 2440 Geel, Belgium*

(Received 7 March 2018; revised manuscript received 25 July 2018; published 28 September 2018)

We report here very precise measurements of the spontaneous fission branching ratio for the ^{240,242}Pu and ^{252}Cf isotopes, performed with a new kind of active scintillating target. It is shown that the method itself leads to unprecedentedly small uncertainties, and that these uncertainties are negligible compared to uncertainties on the isotopic content of the sample. Besides this capability we discuss the possibility to use this kind of detector for the systematic study of charged particle radioactivity, i.e., spontaneous fission, α decay, and heavy-ion radioactivity.

DOI: 10.1103/PhysRevC.98.034612

I. INTRODUCTION

Measurements of spontaneous fission half-lives are very important both for fundamental aspects and for applications of nuclear fission. For the heaviest nuclei spontaneous fission is an important decay process, and eventually may be the most important compared to α decay [1]. Hence this is a key process for predicting superheavy elements stability. Its knowledge is also very important in order to describe nucleosynthesis [2]. Moreover spontaneous fission represents a simple way to study the nuclear fission process, and numerous experiments were performed with ^{252}Cf whose spontaneous branching ratio is about 3%. Some of these experiments aimed at characterizing fission fragments mass or/and charge distributions, while others focused on the neutron or γ-ray emission by fission fragments. All these experiments were performed in order to improve our understanding (energy sharing, deformations, and dynamics, etc.) of the fission process. Spontaneous fission has also been widely used to produce neutron-rich nuclei in order to study their structure [3]. Additionally spontaneous fission is used in experiments as a reference, for example for prompt fission neutron spectra measurements [4,5], or for induced neutron fission cross-section measurements [6].

Fission half-lives are one of the most complicated observables to calculate, since they are very sensitive to the whole detail of the potential energy surface from the ground state to the scission point, and to dynamical effects. Typical uncertainties on fission barrier heights leads to orders of magnitude variations on the spontaneous fission half-life [7]. This is true for the inertia tensor too, which is a key ingredient for the dynamical aspect of the process [8].

We present here an innovative method for such measurements based on a new kind of active target, which leads to very high precision. In a first step we will detail the experimental procedure from sample preparation to α-decay and spontaneous fission measurements. Then we will present the data analysis and the final results for the three isotopes ^{240,242}Pu and ^{252}Cf. Finally we will discuss the uncertainties in order to demonstrate the ability of the method to obtain even more precise measurements. Beyond this work we discuss the possibility to use this method for systematic studies of SF, α decay, and heavy-ion radioactivity.

II. EXPERIMENT DESCRIPTION

A new kind of active liquid scintillating target has been used for the measurements [9]. This detector implements the usual method of liquid scintillation counting (LSC) [10], which consists in loading a liquid organic scintillator with the isotope to be measured. One of the great advantages of this technique is that the isotope is located in the active volume of the detector, and we have demonstrated in Ref. [9] that count losses for α decay are less than one percent, and for fission events losses are extremely small (about 10^{-4}%), and can be neglected. Hence very precise counts can be performed and ratio of α decay to spontaneous fission half-lives can be determined.

The scintillator loading is performed through a liquid-liquid extraction [11]. The actinide is dissolved in a first step into an acid solution. It is then extracted into a scintillating liquid thanks to an extracting molecule HDEHP dissolved at a concentration of 0.05 M. First of all this method is a chemical separation method. Hence, in a single step the isotope of interest can be separated from other elements, and dissolved into the scintillator. The extraction was carried out from 0.5 M HNO_3 in case of plutonium isotopes while a HNO_3 pH 3 solution was used for the extraction of californium [12]. Each extraction was achieved in 15 mL PyrexTM tubes (18×100 mm). The extractions were achieved according the following procedure:

(i) The desired activity of Pu and Cf isotopes was added in 5 mL of 1 M or 10^{-3} M HNO_3 solution
(ii) 1.5 mL of the scintillating mixture (HDEHP 16 g.L^{-1}+ organic liquid scintillator) was added in each tube.

*Corresponding author: gilbert.belier@cea.fr

(iii) The tubes were shaken for 5 min then centrifuged at 2000 rpm for 10 min.
(iv) 1 mL of the organic phase was taking off for measurement.

This chemical separation was mandatory in the case of ^{242}Pu because it needed to be separated from ^{241}Am originating from the ^{241}Pu β^- decay. HDEHP is an efficient molecule for a one-step Pu/Am separation. Indeed, the coefficients of distribution for both radionuclides in 0.5 M HNO_3 are 10^4 and about 0.1, respectively [13]. It leads to a complete extraction of plutonium into the organic phase whereas americium remains in the aqueous phase. In order to control the quality of the chemical separation, γ spectrometries were realized before and after the liquid-liquid extraction, in order to measure the 59 keV γ-ray originating from the ^{241}Am α decay. This spectrometry was performed with a CdTe detector, hence the Compton background under this γ peak was very low. In the spectra obtained after the liquid-liquid extraction the ^{241}Am decay could not be observed despite a high sensitivity.

Once the actinide has been dissolved into the liquid scintillator, the solution is sealed into a quartz test tube, which is then placed inside a lightproof setup composed of a light reflector and of a Hamamatsu R6231 photomultiplier (PMT). The optical link between the test tube and the PMT was guaranteed by filling the internal volume with an optical-grade silicone oil. The PMT anode signal was sampled at 500 Ms s^{-1} with a numerical data acquisition system FASTER [14]. The numerical signal is treated by a numerical measurement module implemented into a FPGA, which provides constant fraction triggering, baseline stabilization, and charge integration. For every event, three charges were stored, and were used for pulse shape discrimination (PSD). It relies on the fact that liquid organic scintillators exhibit 2 fluorescence components, a prompt one referred to as fast, and a delayed one referred to as slow, whose proportions depend on the detected particle. For light charged particles, the higher the mass, the higher the proportion of the slow component. In the charge integration method, these proportions are obtained by integrating the signal over a prompt time gate (fast charge Q_f), and a delayed one (slow charge Q_s). Typical integration times used in the present measurement were, respectively, 10 and 235 ns. For each event a PSD parameter was obtained by computing the ratio $r = Q_s/Q_f$. In addition a third charge Q_{tot} was stored in order to measure the total charge of the signal. Its duration was typically at least 250 ns.

Figure 1 shows a two-dimensional (2D)-identification histogram obtained by plotting this r ratio against the total charge of the signal, in the case of the ^{242}Pu sample. It demonstrates the ability of organic liquid scintillators to identify different kinds of events: α (red peak) and β decays, secondary electrons, fission events. One can see that this PSD method is also able to identify piled events (α-β pileup, α-α pileup, and 3α pileup in the case of ^{242}Pu). We will discuss in the next section how these events are accounted for. The ^{240}Pu and ^{242}Pu samples provided by the JRC.G.2 laboratory at Geel, Belgium [15] were dissolved into the commercial EJ309 scintillator [16], whereas the ^{252}Cf sample was extracted into a homemade Di-Isopropyl-Naphthalene-based scintillator. The

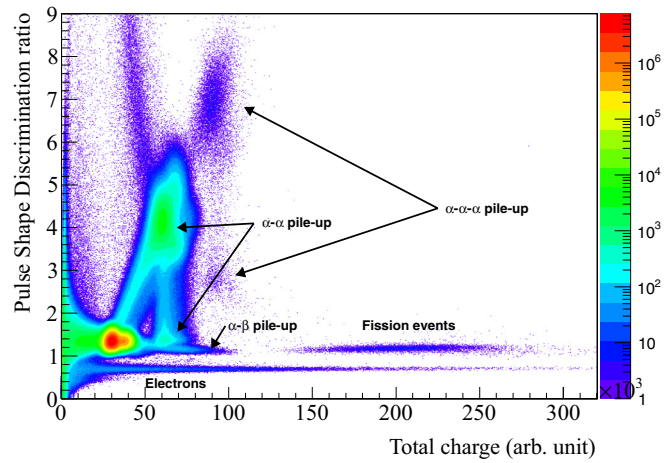

FIG. 1. Identification 2D histogram obtained from the total charge of the signal (x axis) and the ratio of the slow charge over the fast charge (y axis), for the ^{242}Pu sample. The most intense peak (in red) is the α-decay peak.

principal characteristics of the three prepared samples are given in Table I. The two plutonium samples were characterized very precisely in Ref. [15]. In the case of ^{252}Cf the isotopic content certificate furnished by the supplier was used. The main pollution in activity was coming from the ^{250}Cf isotope whose content was 15.591% at the reference date. The cooling time was typically 3.5 years and the ^{250}Cf activity was about 9%.

In the case of ^{252}Cf the given purities are indicative since the measurements lasted 73.5 days. In the following analysis, the decay of every isotope during the three measurements was taken into account. The uncertainties on the isotopic composition for the two plutonium isotopes [8] were propagated. For the three samples the proportion of α activity from ^{240,242}Pu and ^{252}Cf were respectively 94.857, 88.981, and 96.06%. For the two plutonium isotopes the remaining activity was mainly due to the 238 isotope. Since the typical energy resolution of organic liquid scintillators is about 5% for 5 MeV α particles, the ^{238}Pu activity could not be separated from the whole activity, and had to be subtracted from the known ^{238}Pu content. For each measurement, all the events were stored in order to extract precisely the ratio of spontaneous fission over α-decay rates, thus avoiding dead-time corrections. This was especially important for the ^{240}Pu measurement because of its activity and about 15 To of data were stored.

III. DATA ANALYSIS AND RESULTS

From Fig. 1 one clearly see that fission events located at the highest total charges and at PSD ratios intermediate

TABLE I. Mains characteristics of the three prepared samples.

Isotope	Isotopic purity (%)	Activity (Bq)	Fission rate (fission.s^{-1})	Half-life (years) [17]
^{240}Pu	99.89	70×10^3	4×10^{-3}	6561(7)
^{242}Pu	99.96	1.2×10^3	0.06	$3.73(3)\times10^5$
^{252}Cf	65.647	7.3	0.23	2.645(8)

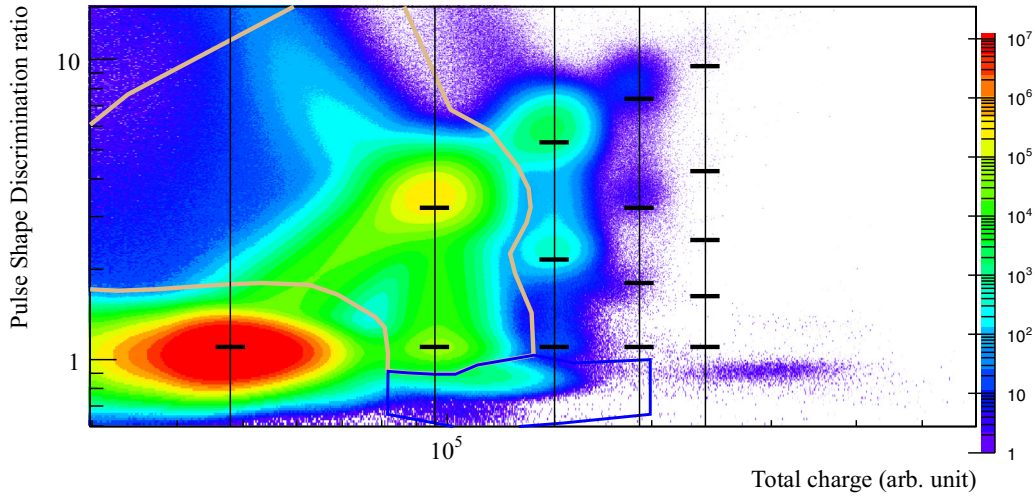

FIG. 2. Identification 2D histogram obtained for the ^{240}Pu sample.

between α particles and electrons, are clearly separated from other type of events. Thus they can be easily counted, to obtain total fission rates for each sample, with only statistical uncertainties. Nevertheless in these total fission rates one has to take into account the spontaneous fission of contaminating isotopes in the samples. For ^{240,242}Pu and ^{252}Cf samples their respective fission rate proportions were calculated to be 99.79, 99.96, and 100% from the known isotopic contents. The propagation of the known composition uncertainties for the plutonium samples has shown that they could be neglected in the final analysis.

Concerning α decays, piled events have to be characterized in order to obtain the total decay rate. These piled events are clearly identified on Fig. 1 for ^{242}Pu, but are even more pronounced for ^{240}Pu as seen in Fig. 2. Up to five piled α-particle events are observed. Vertical lines are plotted to locate multiples $Q_{\text{tot}} = n.E_\alpha$ of the α-peak energy E_α, where n is the number of piled α particles. For $n = 2$ one mainly see two peaks for two different PSD ratios. The first one is located at a ratio equal to r_α (α-peak ratio), and corresponds to almost perfect pileup where the particles almost coincide in time. The second one is located approximately at a ratio given by $1 + 2r_\alpha$, and corresponds to a second α particle that piles onto the slow component of the first one. Obviously this second one is more probable than the first one, since the slow component is longer than the fast one, and a simple calculation of chance coincidences reproduces well the rates of the two peaks. Intermediate chance coincidences are also observed leading to partial energy loss and/or intermediate r ratios.

More generally for n piled α particles, n peaks should appear. Obviously the first coordinate is given by:

$$Q_{\text{tot}} = n.E_\alpha.$$

If $m \in [1, n]$ is the number of α particles almost in perfect coincidence the associated ratio is given by:

$$r = \frac{m.Q_s + (n-m)Q_{\text{tot}}}{m.Q_f}.$$

That simplifies to:

$$r = (1 + r_\alpha)^{n}\!/_{m} - 1.$$

Horizontal lines are plotted in Fig. 2 in order to locate all these peaks up to $n = 5$. The positions of the different peaks are relatively well reproduced, hence the pattern of this histogram is qualitatively explained. Finally the number of piled α particle is easy to determine in this 2D histogram. An important feature in such analysis is that for the highest pileup order, i.e., $n = 4,\ 5$ one would have a significant overlap with fission events, with conventional analysis looking only the total charge. However, here the PSD method allows a clear separation of these events. This has nothing to do with the PSD capability of organic liquid scintillators, and the method can also be used with conventional detectors such as fission chambers.

Once the pileup order is determined it is straightforward to define graphical cuts in order to extract the statistics. In Fig. 2 the graphical cut used to extract the statistic N_2 of double α-α pileup ($n = 2$) is plotted (orange contour). We do not plot every cut for sake of clarity, but N_n, for $n = 1$–5, is extracted identically. Finally the total number of α decay N_α is obtained by summing all contributions:

$$N_\alpha = \sum_n n\ N_n \quad n \geqslant 1.$$

For N_1 α-electrons coincidences were taken into account by just adding the number of counts extracted from the α-electron pileup graphical cut (blue contour in Fig. 2). Still for N_1 an extra correction was applied in order to take into account the escape of α particles at the scintillator border, which lead to count losses. As already mentioned the statistic in the α peak represents 99.4% (losses amount to 0.6%). Nevertheless the graphical cut includes events in the tail (partial energy deposit) and the detection efficiency is higher. In fact losses were calculated to be 0.1, 0.16, and 0.06%, respectively, for ^{240,242}Pu and ^{252}Cf isotopes. They were obtained by extrapolating the α-peak tail at the lowest energies where α particles and electron can not be completely separated. The values of the α-particle detection efficiencies correlate very well to the

TABLE II. Spontaneous fission branching ratio.

Isotope	SF branching ratio	Uncertainty (%)
^{240}Pu	5.796(39).10^{-8}	0.68
^{242}Pu	5.510(41).10^{-6}	0.74
^{252}Cf	3.1028(27).10^{-2}	0.09

energies, which are, respectively, at 5156, 4896, and 6112 keV (weighted averages). Moreover polynomials of order 1 and 2 were tested for the extrapolation, and it was shown that losses changes were very small. Finally the associated uncertainties were neglected.

The branching ratio for spontaneous fission b_{SF} is given by:

$$b_{SF} = \frac{1}{1 + N_\alpha / N_{SF}}.$$

where N_α and N_{SF} are, respectively, the number of α decay and spontaneous fission. This branching ratio is given for all isotopes in Table II with the absolute uncertainties (second column) and the relative uncertainties (third column).

In order to discuss the method we give in Table III. the uncertainty budget for the measurement performed on the ^{240}Pu sample. It can be seen that the uncertainty on the α-particle detection efficiency, as discussed previously, is negligible compared to other terms. The two following terms are related to the graphical cuts used to extract the statistics on the number of unpiled α decay, and doubly piled α-α decays. All the cuts are traced by hand, thus introducing a subjective uncertainty. In order to quantify this, the cuts were changed in order to obtain more or less permissive cuts. The maximum change in statistics was used to estimate the associated uncertainties, which turn out to be small. The next term is the content activity uncertainty. It is associated to the isotopic content of the sample, and is obtained by propagating the associated uncertainties measured at a reference date, and from the different isotopes half-lives uncertainties, since the cooling for every isotope has to be calculated. Finally the last and the largest term is the statistical uncertainty on the number of fission events. This last one is not an absolute limit since the measurement could be longer, hence the most limiting factor in these measurements are the precisions on the sample isotopic purity. Every uncertainty coming from the method itself is much lower, and we can conclude that the method does not limit the attainable precisions.

TABLE III. Uncertainty budget for the measurement on ^{240}Pu.

Uncertainty origin	value
α detection efficiency	0.01%
α count	0.04%
α-α pile-up	0.04%
Activity content	0.12%
Fission statistic	0.67%
Total	0.68%

For comparison purpose we give in Table IV the spontaneous fission half-lives T_{SF}, that are easily obtained from the branching ratio and the isotope half-life $T_{1/2}$ through:

$$T_{SF} = \frac{T_{1/2}}{b_{SF}}.$$

The second column gives the spontaneous fission half-life by propagating the branching ratio uncertainty only, while in the third one the uncertainty on the isotope half-life is included. Surprisingly for ^{252}Cf the half-life uncertainty is by far the most important one, while this is a well-known nuclei, which has been used in numerous experiments. In the fourth column we give the evaluated data published by Holden [18] and in the last column the experimental reference, which is the most precise measurement obtained (Ref. [19] for the plutonium isotopes, and Ref. [20] for californium). We can conclude that our measurements are the most precise for the plutonium isotopes, even compared to the evaluated data, which combines several measurements. Of course for californium there is no gain to expect, but still the branching ratio is very precise.

IV. DISCUSSION

The decisive advantage of the LSC technique described here is to allow very precise counts of α decays and fission events. This is due to the fact that the actinide is dissolved into the active volume of the detector, and that losses are encountered in a very small volume at the liquid borders, defining a skin. The thickness of this skin is the particle range, which is typically 50 μm for α particles and 20–30 μm for fission fragments. Since in fission events there are two fragments this is very unlikely to lose the two fragments. Hence as already mentioned α-decays losses range between 0.06 and 0.16%, and the fission counts losses amount to about 10^{-4}%. For these first ones, corrections can be applied with negligible uncertainties. It has been demonstrated that the main uncertainty associated to this technique is 0.04% and is due to α-α pileup. This represents the limitation of the actual setup, and this limitation can be pushed down since we did not perform a true pileup rejection, nor a pileup treatment based on waveforms analysis. The next terms related to the α-particles detection efficiency can be optimized also, since a usual geometry was used in this work. In fact this can be easily obtained by using a larger volume of liquid scintillator. For example 100 mL is a reasonable volume for a liquid scintillator detector and the α count losses would be 100 times lower than the actual value since the liquid volume is typically 1 mL. Hence α count losses would be at the level of 10^{-3}% with extremely small uncertainties. This discussion shows that the method can be optimized in order to reach higher precisions, and higher activities. In practice the precisions are limited by the uncertainties on the isotopic impurities in the sample, and the limits imposed by the detector itself are not attained.

The LSC method can be compared to usual methods that are used for fission and α-decay counting. One can cite the use of Frisch gridded fission chambers as the one used in Ref. [19] for the most precise measurements of SF on

TABLE IV. Spontaneous fission half-lives in years.

Isotope	This work		Holden	Experimental ref
^{240}Pu	$1.132(8)\times10^{11}$	$1.132(8)\times10^{11}$	$1.140(10)\times10^{11}$	$1.165(13)\times10^{11}$
^{242}Pu	$6.77(5)\times10^{10}$	$6.77(7)\times10^{10}$	$6.77(6)\times10^{10}$	$6.74(9)\times10^{10}$
^{252}Cf	85.245(75)	85.24(27)	86(1)	85.54(22)

^{240}Pu and ^{242}Pu prior to ours. Geometry-defined solid-state detector systems can also be used [21] and more occasionally mass spectrometer [22]. Contrarily to the LSC, these three methods require the preparation of a thin and uniform deposit. This step is time consuming and demands a strong expertise together with dedicated equipment. This also introduces a severe limit on the mass sample since fission fragments have small ranges, which limits the sample thickness to a maximum of $100\,\mu$g.cm^{-2}. This is mandatory to separate α particles from fission fragments and especially in 2π geometry setups, such as in Frisch gridded fission chambers. This aspect is less crucial for low solid angle geometries, because detected fission fragments emitted perpendicular to the sample have the minimum energy loss in the deposit. These low solid angle setups can be extremely precise too, but this is at the expense of the detection efficiency, and thus of the counting rate. Hence the LSC method allows extremely precise counts, together with unlimited mass. The mass limit will be solely due to pileup effects but here again liquid organic scintillators have a definitive advantage since fluorescence characteristic times are few nanoseconds.

The high-precision measurements that were discussed in this work are very important for nuclear data needed in nuclear applications. The ^{242}Pu branching ratio has already been used in a neutron fission cross section measurement, in order to determine the fission fragment detection efficiency of a fission detector [6]. On the contrary these precisions do not help to understand the fission process itself, since the theoretical models are far from reproducing precisely the spontaneous fission half-lives. The main goal for these models is to predict at least the half-lives orders of magnitude. Beyond precision, the possibility to perform systematic measurements in order to map the nuclear mass table is something important in order to test the ability of models to predict decay modes. In this work we have shown that LSC counting can be used easily to reach a precision of 0.68% on a branching ratio of 5.796×10^{-8} in a counting experiment that lasted 60 days on ^{240}Pu. If the targeted precision is only 10% one would have been able to measure a branching ratio as low as 2.7×10^{-10} in the same conditions (counting time and sample activity). This value is indicative and does not represent an absolute limit, but it shows that the method can be used for isotopes with low SF branching ratios. This is the case for some actinides such as ^{231}Pa, ^{230}U, or ^{237}Np for which only limits on SF half-lives are given [23]. Of course for higher Z, spontaneous fission is becoming more and more likely, and more and more isotopes remains to be measured. At this level of sensitivity, the heavy particle radioactivity (HPR) can be measured too. For example ^{14}C radioactivity of ^{223}Ra, would have been detected (100 events) in about one month with a 70 kBq sample, while Rose and Jones [24] used a 167 kBq during more than six months to obtain 11 events. In fact much lower branching ratio can be reached with the LSC technique, and Mg or Ne radioactivity, for example, can be measured. The sensitivity of the LSC method, together with the ease of the scintillator preparation (equipment needed and preparation duration), allows extended studies of α, heavy-ion radioactivities, and SF. Such systematic measurements might be important for an overall understanding of charged particle radioactivity. One can cite the superasymmetric fission model that treats both HPR and SF [25], and that was used recently to predict a HPR of superheavy elements (SHEs) [26]. Recently great progress was obtained in microscopic HFB calculations performed with the D1M energy density functional, in the reproduction of SF half-lives [27].

ACKNOWLEDGMENTS

This work was supported by the ANDES Collaborative project FP7-249671 of DG-RTD, the European Commission's Directorate General for Research and Innovation.

[1] Y. Oganessian, J. Phys. G **34**, R165 (2007).
[2] S. Goriely, J.-L. Sida, J.-F. Lemaître, S. Panebianco, N. Dubray, S. Hilaire, A. Bauswein, and H.-T. Janka, Phys. Rev. Lett. **111**, 242502 (2013).
[3] A. V. Ramayya, J. H. Hamilton, and J. K. Hwang, J. Phys.: Conf. Ser. **580**, 012017 (2015).
[4] R. Capote *et al.*, Nucl. Data Sheet **131**, 1 (2016).
[5] A. Chatillon, G. Bélier, T. Granier, B. Laurent, B. Morillon, J. Taieb, R. C. Haight, M. Devlin, R. O. Nelson, S. Noda, and J. M. O'Donnell, Phys. Rev. C **89**, 014611 (2014).
[6] P. Marini, L. Mathieu, M. Aïche, G. Bélier, S. Czajkowski, Q. Ducasse, B. Jurado, G. Kessedjian, J. Matarranz, A. Plompen, P. Salvador-Castiñeira, J. Taieb, and I. Tsekhanovich, Phys. Rev. C **96**, 054604 (2017).
[7] A. Baran, M. Kowal, P.-G. Reinhard, L. M. Robledo, A. Staszczak, and M. Warda, Nucl. Phys. A **944**, 442 (2015).
[8] F. P. Heßberger, Eur. Phys. J. A **53**, 75 (2017).
[9] G. Bélier, J. Aupiais, C. Varignon, and S. Vayre, Nucl. Instrum. Methods Phys. Res. A **664**, 341 (2012).
[10] R. Broda, P. Cassette, and K. Kossert, Metrologica **44**, S36 (2007).
[11] N. Dacheux and J. Aupiais, Anal. Chem. **69**, 2275 (1997).
[12] N. Dacheux and J. Aupiais, Anal. Chim. Acta **363**, 279 (1998).

[13] G. H. Coleman, *The Radiochemistry of Plutonium*, NAS-NS 3058, Washington, DC, 1965.
[14] http://faster.in2p3.fr
[15] G. Sibbens *et al.*, J. Rad. Nucl. Chem. **299**, 1093 (2014)
[16] ELJEN Technology http://www.eljentechnology.com
[17] http://www.nndc.bnl.gov
[18] N. E. Holden and D. C. Hoffman, Pure Appl. Chem **72**, 1525 (2000).
[19] P. Salvador-Castineira, T. Brys, R. Eykens, F. J. Hambsch, A. Moens, S. Oberstedt, G. Sibbens, D. Vanleeuw, M. Vidali, and C. Pretel, Phys. Rev C **88**, 064611 (2013).
[20] M. R. Schmorak, Nucl. Data Sheet **32**, 87 (1981).
[21] S. Pommé and G. Sibbens, Acta Chim. Slov. **55**, 111 (2008).
[22] S. Gales, E. Hourani, M. Hussonnois, J. P. Schapira, L. Stab, and M. Vergnes, Phys. Rev. Lett. **53**, 759 (1984).
[23] National Nuclear Data Center https://www.nndc.bnl.gov
[24] H. J. Rose and G. A. Jones, Nature (London) **307**, 245 (1984).
[25] D. N. Poenaru, M. Ivaşcu, A. Sndulescu, and W. Greiner, Phys. Rev. C **32**, 572 (1985).
[26] D. N. Poenaru, R. A. Gherghescu, and W. Greiner, Phys. Rev. Lett. **107**, 062503 (2011).
[27] A. Giuliani, L. M. Robledo, and R. Rodriguez-Guzman, Phys. Rev. C **90**, 054311 (2014).